https://doi.org/10.2352/CIC.2025.33.1.4

Skin color preference under multi-scene demand

Beijia Qin[1], Yuechen Zhu*, and Ming Ronnier Luo[1]

[1]State Key Laboratory of Extreme Photonics and Instrumentation, Zhejiang University, Hangzhou, China

****Corresponding Author: zhuyuechen@zju.edu.cn***

Abstract

This study discusses how scenes and model's appearance, gender and makeup status influence the preference facial skin tone of Chinese models for Chinese observers. This research also explores how the models' preference differ from the stranger observers. The results show that the makeup status can affect the scope of the preference area. The preference centers exhibit a trend of higher lightness and smaller hue angles than original ones. In all scenes except indoor scenes, a higher CCT correlates with a greater inclination angle of the ellipsoid projection on the a^*-b^* plane, a narrower ellipsoid range, and a smaller hue angle of the ellipsoid center. Apart from the in-lab scenario, higher scene color temperatures are associated with a larger chroma increment and a smaller hue increment in the preference centers relative to the original image skin tones. Also, the chroma of the preference centers of indoor and in-lab scenes is lower than that of the original images, distinguishing them from other scenes. The models' preference is influenced by their actual skin color to a larger extent.

Introduction

Skin tone preference plays a critical role in preferred color enhancement. Extensive research has shown that observers exhibit a preferred skin color center, with studies indicating that shifting skin tones toward this center enhances perceptual satisfaction. Early investigations by Bartleson [3, 4], Sanders [5], and Hunt et al. [6] focused on Caucasian skin tones, revealing that preferred hues tend to be yellower and more chromatic than actual skin colors. Sanger et al. [7] expanded this to multi-ethnic comparisons, finding that preferred chroma increases sequentially in Caucasian, Mongoloid, and Negroid groups while hue angles remain consistent. Zeng and Luo's cross-ethnic experiments [11] converged on a preferred hue angle of 49° in CIELAB. Peng et al. [12] found similarities in chroma and hue but variations in lightness. Cao et al. [13] found that high-CCT illuminants are favored with slight chroma adjustments. Luo [14] introduces the Preferred Memory Color (PMC) chart, a 30-patch tool for evaluating color reproduction quality, integrating preferred memory colors, gamut boundaries, and grayscale for imaging and lighting applications.

While extant research has established a comprehensive framework, it is revealed concurrently that skin color preference could be affected by model characteristics and observer demographics. The focus of this study includes the gender and makeup status of the models and the relationship between strangers' skin tone preferences and models' self-perceptions.

Experimental

Database collection

A data set including laboratory standard environment images and outdoor images was established. Skin color data measured on each model's forehead, left cheek, right cheeks, nose tip and chin was collected with a Konica Minolta CM-700d Spectral colorimeter [15]. The L'Oréal Skin Color Chart [16] classification is used as a reference. A total of 9 models, including 4 men and 5 women, were used, among which female models were collected separately with and without makeup. The skin colors data of 9 models in CIE $L^*a^*b^*$ space is shown in Figure 2, along with the L'Oréal skin color classification and ITA type [17] of each model's skin color measurement results.

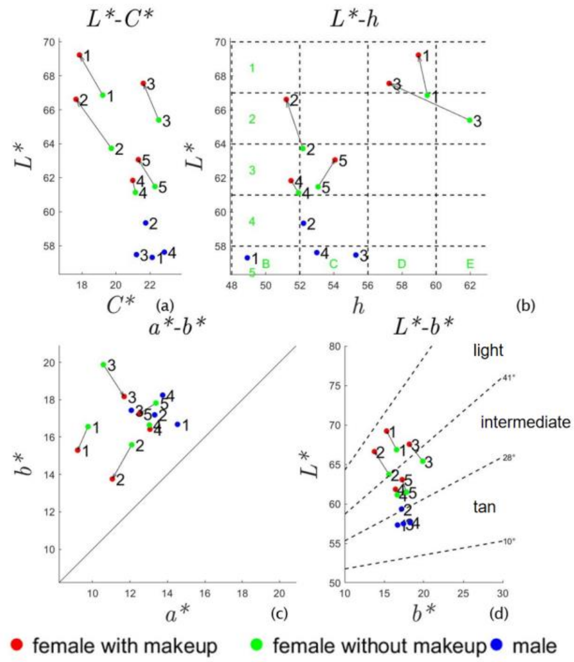

***Figure 2**. Skin color data of the nine models measured by a spectral colorimeter. (a) L^* versus C_{ab}^*. (b) L^* versus h_{ab}. The green numbers and letters indicate the lightness and hue scale of the L'Oréal skin color classification. (c) a^* versus b^*. (d) L^* versus b^*. The dividing lines between ITA classifications are plotted.*

It can be noticed that for female models' skin color, and the lightness is higher and the chroma is lower after makeup, and the skin color of male models is generally lower in lightness and higher in chroma than that of female models.

The laboratory standard environment data set was collected by HasselbladX2D 100C camera [18] and a mobile phone. The light condition with 7000k color temperature and 500 lx illuminance is used in this experiment. The model sat in the light source room illuminated by two rows of Thouslite LEDcube [19] lightboxes. Figure 1 shows the image capturing condition.

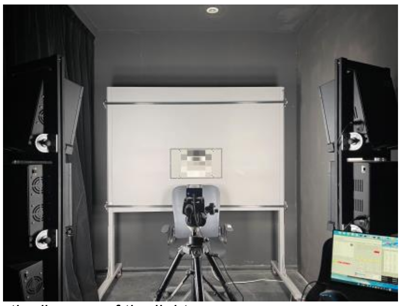

Figure 1. Schematic diagram of the lightsource room.

The real-scene image set includes 4 types of scenes, which are indoor, outdoor, night and sunset separately. The number of the images of each scene type is 10, 10, 10 and 4 separately. The models used for the real scene database are male models No.1, 2, 3 and 4 and female models No.3, 4 and 5.

Figure 3 and Figure 4 show images used in-laboratory and real-scene experiment respectively.

Figure 3. Original images of the indoor images. (a) Female No.1 with makeup; (b) Female No.1 without makeup; (c) Female No.2 with makeup; (d) Female No.2 without makeup; (e) Female No.3 with makeup; (f) Female No.3 without makeup; (g) Female No.4 with makeup; (h) Female No.4 without makeup; (i) Female No.5 with makeup; (j) Female No.5 without makeup; (k) Male No.1; (l) Male No.2; (m) Male No.3; (n) Male No.4.

Figure 4. Examples of original images of real scene images. (a)Female No.4 in Indoor scene; (b) Female No.4 in night scene; (c) Female No.4 in outdoor scene; (d) Female No.4 in sunset scene; (e)Male No.1 in Indoor scene; (f) Male No.1 in night scene; (g) Male No.1 in outdoor scene; (h) Male No.1 in sunset scene.

Display

A Konica Minolta CS2000A [20] spectroradiometer is used for display characterization of the two mobile phones used in this experiment. A 9-9-9 3D-LUT model was built, with the 729 and 96 sets of color blocks being the training and verifying samples respectively, and the XYZ values measured by CS2000A spectroradiometer. The forward and backward performance of the model evaluated in CIEDE2000 [21, 22] is shown in Table 2.

Table 2: The average, maximum, minimum and standard deviation of forward and reverse color difference (CIEDE2000) of the 3D-LUT model on the two mobile phones

		mean	*max*	*min*	*std*
forward	No.1	0.65	1.40	0.14	0.71
	No.2	0.62	1.22	0.10	0.79
backward	No.1	0.42	1.10	0.08	0.27
	No.2	0.41	0.94	0.10	0.28

Image Rendering

A 49 points pattern is used according to previous studies [23, 24]. The coordinates of the pre-select points relative to the statistical average center of the skin color pixels are shown in Figure 5.

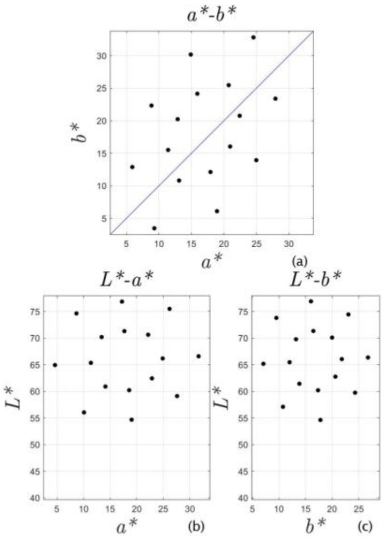

Figure 5. Rendering Pattern. (a) Points on a-b* plane; (b) Points on L*-a* plane. (c) Points on L*-b* plane.*

The color of pixels that are covered by the skin mask is shifted according to Equation (1), where L^*, a^* and b^* are the original CIE $L^*a^*b^*$ values of skin color pixels , ΔL^* , Δa^* and Δb^* are the relative CIE $L^*a^*b^*$ values of the 49 pre-selected points, L^*_{new} , a^*_{new} and b^*_{new} are the $L^*a^*b^*$ values of the skin color pixels after rendering.

$$\begin{aligned} L^*_{new} &= L^* + \Delta L^* \\ a^*_{new} &= a^* + \Delta a^* \\ b^*_{new} &= b^* + \Delta b^* \end{aligned} \quad (1)$$

Experimental Procedures

The experiment was conducted in a darken room shown as Figure 6. The display was placed about 40 cm away perpendicular to the observer's eyes.

Figure 6. Experimental situation.

Each original image generates 54 images (49 reproductions, with a 10% repetition rate). The number of images in each part is 14 * 54 = 756 (in-lab), 10 * 54 = 540 (indoor), 10 * 54 = 540 (night), 10 * 54 = 540 (outdoor) and 4 * 54 = 216 (sunset) respectively. In total, (756 (in-lab) + 540 (indoor) + 540 (night) + 540 (outdoor) + 216 (sunset)) (judgements including repetition) * 20 (observers) = 51840 sets of data is collected. If one judgement is estimated to take 3 seconds, then it takes ((54 (judgements within one set of rendering) * 3 (time taken by one judgement) * 14 (rendering sets)+ 20 (adaptation time between two groups)) * 13 (intervals) + 60 (adaptation time at the beginning))= 2588 seconds = 43.13 minutes to finish the in-lab part, and through the same calculation we can obtain the periods taken by the rest parts of the experiment which are 31 minutes for each part of indoor, night and outdoor and 12.8 for the sunset part. The experiment takes each observer (43.13 (in-lab) + 31 (indoor) + 31 (night) + 31 (outdoor) + 12.8 (sunset)) = 148.93 minutes = 2.48 hours.

All observers passed Ishihara color blindness test and had normal vision without color blindness or color weakness.

The experimental interface is shown in Figure 7. There is a 60-second adaptation time before the experiment starts, and a 20-second adaptation time between two groups of 54 images. The experiment used a six-scale evaluation method [25] with a Bluetooth keyboard. The white text shows the serial of the current image and the total number of the images.

Figure 7. Experimental interface.

Results and Discussions

Observer Variations

The standardized residual sum of squares (STRESS) [27] which is calculated by Equation (2) was used to test the repeatability within and between subjects.

$$STRESS = \sqrt{\frac{\sum_{i=1}^{n}\left(A_i - FB_i\right)^2}{\sum_{i=1}^{n}F^2B_i^2}} \times 100 \qquad (2)$$

Where $F = \frac{\sum_{i=1}^{n}A_i^2}{\sum_{i=1}^{n}A_iB_i}$. The value of n represents the count of sample pairs, while F serves as a multiplier to harmonize the scales of datasets A and B. The average, maximum, minimum and standard deviation of STRESS within and between subjects in the experiment are shown in Table 3.

Table 3. The average, maximum and minimum value and standard deviation of intra STRESS and inter STRESS

.	*mean*	*max*	*min*	*std*
Intra STRESS	0.19	0.27	0.12	0.04
Inter STRESS	0.37	0.46	0.29	0.05

The average STRESS within the subjects is 0.19, which means that the repeatability within the subjects is reliable, and the average STRESS between the subjects is 0.37, which is comparable to similar studies[12].

Preferred skin tone ellipsoids

The data processing flow is shown in Figure 8. For the $L^*a^*b^*$ value used in the experiment, firstly, it is converted to XYZ space with the white point of the display, and then chromatic adaptation transform (CAT) [28] is performed on it, where the formula of the D is calculated by the formula of CAT16. Next, it is transformed into CIE $L^*a^*b^*$ space with D65 reference white for subsequent fitting. For the data generated in the experiment, firstly, it is converted into z-score [29, 30], and then used in the subsequent fitting operation.

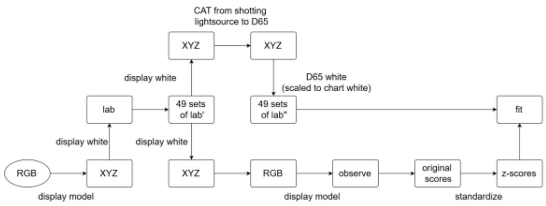

Figure 8. Data processing flow chart.

After the z-score is obtained, the 50% acceptability ellipsoid is fitted using Equation (3).

$$P = \frac{1}{1 + e^{\Delta E' - \alpha}} \qquad (3)$$

Where $\Delta E' = \sqrt{k_1 \cdot \left(L^* - L_0^*\right)^2 + k_2 \cdot \left(a^* - a_0^*\right)^2 + k_3 \cdot \left(b^* - b_0^*\right)^2 + k_4 \cdot \left(a^* - a_0^*\right) \cdot \left(b^* - b_0^*\right)}$

and P is the z-score obtained in the previous step, L_0^* a_0^* b_0^* is the center of the fitted acceptability ellipsoid, k_1 , k_2 , k_3 and k_4 are the fitting parameters. The average correlation coefficient of all ellipses is 0.97, which means that the correlation between the predicted value and the sampled value is good.

An acceptability ellipsoid [12, 31] is obtained from 49 points rendered by each original image. For the centers of acceptable ellipsoids obtained images of each model, a perceptibility ellipsoid is obtained using Equation (4).

$$\left[X - \Psi\right]^T \Lambda^{-1}\left[X - \Psi\right] = r \qquad (4)$$

Where X represents all the sample data points (x_i, y_i), which in this specific case is the fit center of all acceptability ellipsoids of all images of the same model, ψ defines the center of the confidence ellipsoid and is the expected estimate of the sample data points calculated by $\Psi = \frac{1}{n}\sum_{i=1}^{n} X_i$. Λ is the covariance matrix of the sample calculated by $\sigma(x, y) = \frac{1}{n-1}\sum_{i=1}^{n}\left(x_i - \bar{x}\right)\left(y_i - \bar{y}\right)$, and r is calculated by the inverse cumulative distribution function of chi-square distribution obtained by chi2inv(1- alpha,V) where alpha is 0,05 and V equals to 3 as the degree of freedom.

Comparison with previous experimental results

Figure 9 shows a comparison between the projection of 95% perceptibility ellipsoid of the in-laboratory experiment and some previous experiments. It can be seen that the Peng [12] and Cao [13] has a similar hue with that of preference memory color chart (PMCC), which is approximately 46.18°.Result of Zeng et al. [24] has the most similar hue angle(49.40°) with this experiment(50.32°).

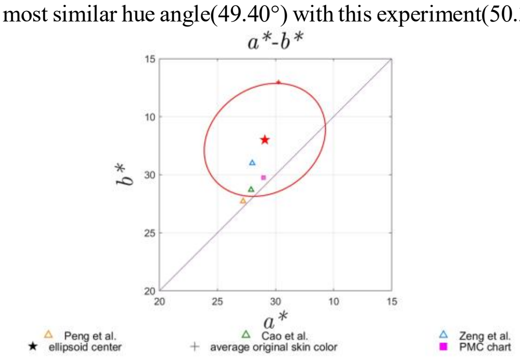

Figure 9. *Comparison with other experiments (projection on a*-b* plane).*

Preferred skin tone affected by the models

This experiment mainly discusses the influence of factors related to the model (including appearance, gender and makeup) and the scene on the skin color on the preference center of Chinese model for Chinese observers, as well as the how the preference of the models themselves differ from the stranger observers.

According to the Mann-Whitney U test [32], the mean value of the p of the pairs is 0.34, indicating that the skin color preference center is independent of the appearance of the models, thus analyzing the influence of scenes without considering the appearance of the models is plausible.

The p values of the Lilliefors analysis [33] of female models and male models are 0.41 and 0.33, which are all greater than 0.05. While the K-S statistics is lower than the critical value in each group, indicating that the two groups of data approximately obey the normal distribution. The ratio of the variance is 1.35, which is greater than 0.5 and less than 2, indicating that the data of the two groups have homoscedasticity. It is considered that the ANOVA analysis [34] is workable. The average p values of the ANOVA analysis in the five dimensions is 0.47, which is larger than 0.05, so it can be considered that the center of the acceptability ellipsoids is almost independent of the gender of the model, and thus it is plausible to exclude the genders of the models as a variable when analyzing the influence of scenes on the preference center.

Figure 10 shows the cross-sections of perceptibility ellipsoids of each gender on a^*-b^*, L^*-a^* and L^*-b^* planes. It can be seen that the center of perceptibility preference ellipsoid of female models has no noticeable deviation from that of male models in hue, but is slightly higher in lightness and slightly lower in chroma.

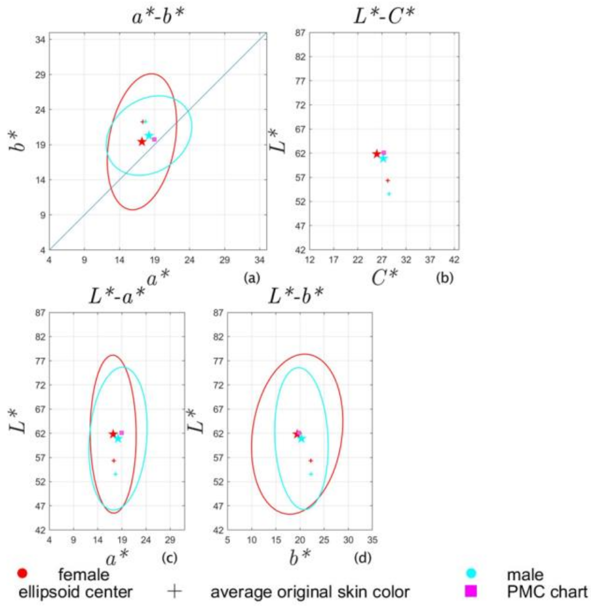

Figure 10. *Sections of 95% perceptibility ellipsoids of different genders. (a)a*-b* diagram; (b)L*-C* diagram; (c)L*-a* diagram; (d)L*-b* diagram.*

The Mann-Whitney U test shows that the p values in L^*, a^*, b^*, C_{ab}^* and h_{ab} five dimensions are separately 1.00, 0.69, 0.69, 1.00 and 0.84, which are all greater than 0.05, indicating that the center of acceptability preference ellipsoid is almost independent of the make-up status.

Figure 11 shows the cross-sections of perceptibility ellipsoids of each scene of on a^*-b^*, L^*-a^* and L^*-b^* planes. Although the perceptibility ellipsoid center of the ellipsoid after makeup is slightly higher in lightness and chroma compared with that before makeup, on the whole, there is no significant difference in the preference center between different makeup status, which means it is plausible to analyze the influence of the scenes without considering the models' makeup status. However, there is an obvious narrowing trend in the scope of the ellipsoid, which can be inferred that the observers' tolerance for women's skin color changes is narrower when the model is wearing makeup.

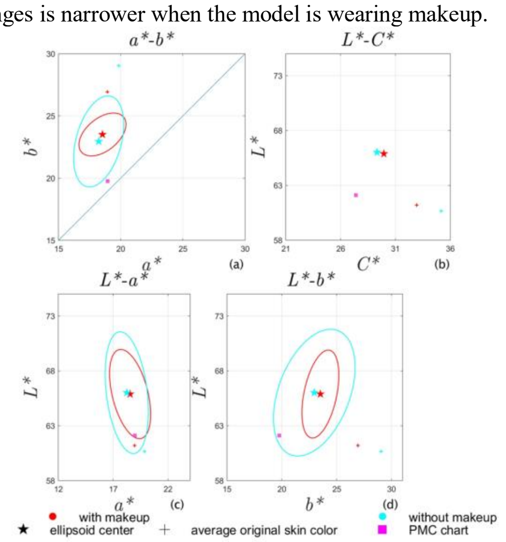

Figure 11. *Sections of 95% perceptibility ellipsoids of different makeup status. (a)a*-b* diagram; (b)L*-C* diagram; (c)L*-a* diagram; (d)L*-b* diagram.*

Preferred skin tone affected by the scenes

Kruskal-Wallis test [35] is carried out on the L^*, a^*, b^*, C_{ab}^* and h_{ab} values of 50% acceptable preference ellipsoid center obtained from different images under all scenes and the results are shown in Table 5.

Table 5. average color difference of the preference centers between and within the scenes

	L*	a*	b*	C*	h
p	0.02	0.00	0.00	0.00	0.01

The results indicate that the influence of the scenes on the 50% acceptability preference ellipsoid centers is significant.

Figure 12 shows the cross-sections of perceptibility ellipsoids of each scene of on a^*-b^*, L^*-a^* and L^*-b^* planes.

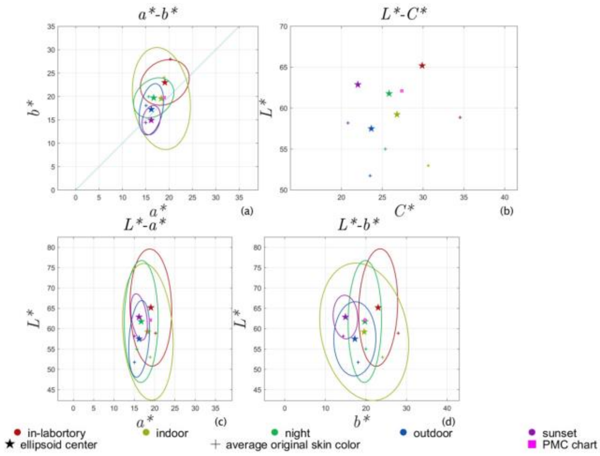

Figure 12. Sections of 95% perceptibility preference ellipsoid center of different scenes. (a)a-b* diagram; (b)L*-Cab* diagram; (c)L*-a* diagram; (d)L*-b* diagram.*

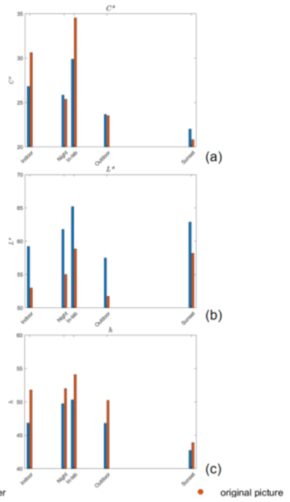

Figure 13. (a)Cab values of each secne; (b) L* values of each secne; (c) h values of each secne.*

Figure 13 shows the C_{ab}^*, L^*, h_{ab} of the center of 95% perceptibility ellipsoid of each scene and the average C_{ab}^*, L^*, h_{ab} of the original skin color region and the average CCT of each scene. The skin colors of original images have already gone through the same processing procedures as the data used to fit the ellipsoids including chroma adaptation transform and the change of the white point.

Firstly, the preference centers show a trend of higher lightness and smaller hue angle than the original image, indicating that observers generally like more light and reddish skin color. Secondly, except for indoor scenes, the higher the color temperature, the greater the inclination angle of the ellipsoid projection on the a^*-b^* plane, the narrower the ellipsoid scope and the smaller the hue angle of the ellipsoid center. Thirdly, except the in-lab scene, the higher the color temperature of the scene, the greater the chroma increment and the smaller the hue increment of the preference center relative to those of the skin color of the original images. Fourthly, for in-lab and inside scenes like in-lab setting and indoor scenes, in contrast to other scenes, the chroma of the preference center is lower than that of the original picture. Thus, it can be inferred that observers may prefer more unsaturated skin color in inside scenes. This may be due to the inside scenes have darker or more complex backgrounds, thus more unsaturated skin color can create contrast with the background and highlight the object.

Self-perception of the models

Figure 14 shows the comparison between $L^*a^*b^*$ values of original images and acceptability preference ellipsoid centers of stranger subjects and models own preference center calculated by the weighted average of the points scored by the model as positive (if there are no points scored as positive, take the weighted average of the points with the highest score).

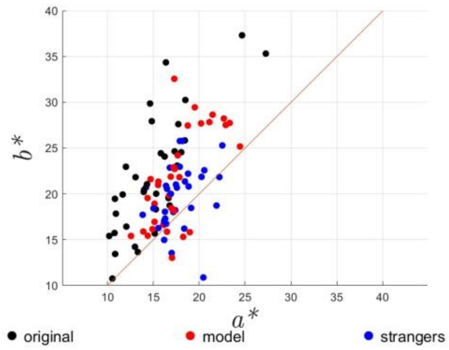

*Figure 14. Comparison between L*a*b* values of original picture (black dots) and acceptability preference ellipsoid centers of stranger subjects (blue dots) and models own average centers (a)a*-b* plane (b) Three-dimensional diagram.*

It can be seen that the $L^*a^*b^*$ value of the original image is relatively decentralized, followed by the preference centers of the models, and the preference centers of the stranger observers is the most concentrated. The average color difference between the preference centers of the models and the original image skin color and between the preference centers of the stranger observers and the original image skin color is 9.14 and 13.63 respectively. It can be inferred that the models' preference is influenced more by their own skin colors than the strangers.

Conclusion

This study systematically investigates the influences of model-related factors (appearance, gender, makeup status) and scenes on the preference when Chinese view portraits of Chinese, finding that the makeup status may narrow the tolerance range for skin color variations. The preference centers tend to be lighter and more reddish than the original ones. In all scenes except indoor environments, a higher color temperature corresponds to a steeper inclination angle of the a^*-b^* plane projection, a more confined ellipsoid range, and a smaller hue angle of the ellipsoid's center. Also, aside from the in-lab scenario, higher scene color temperatures are associated with a larger chroma increment and a smaller hue increment in the preference centers compared to the original image's skin tones. In controlled environments such as in-lab settings and indoor scenes, the chroma of the preference centers is lower than that of the original images, distinguishing them from other scene types. Stranger observers show more concentrated preference centers than models themselves. This study provides results for developing scene-adaptive color reproduction algorithms for imaging devices. Future research could expand to include more ethnic groups and diversify scene datasets.

References

[1] in The Reproduction of Colour. (2004), pp. 31-46.
[2] H. Zeng, R. Luo, Preferred skin color enhancement for photographic color reproduction. IS&T/SPIE Electronic Imaging (SPIE, 2011), vol. 7866.
[3] C. J. Bartleson: "Memory Colors of Familiar Objects*." J. Opt. Soc. Am. 50,73-77 (1960).
[4] C. J. Bartleson: "On the Preferred Reproduction of Flesh, Blue-Sky, and Green-Grass." Photogr. . Eng 6 (1961).
[5] L. Sanders C: "Color Preferences for Natural Objects." Illum. Engng. 54,452-456 (1959).
[6] R. W. G. Hunt, P. I. T., L. M. and Winter: "The Preferred Reproduction of Blue Sky, Green Grass and Caucasian Skin in Colour Photography." The Journal of Photographic Science 22,144-150 (1974).
[7] T. A. Demas Sanger, Hideaki Haneishi, Yoichi Miyake:Facial Pattern Detection and Its Preferred Color Reproduction. In:IS&T 2nd Color and Imaging Conferenceon Proceedings,pp.149 - 153 (1994)
[8] T. Yano, K. Hashimoto: "Preference for Japanese complexion color under illumination." Color Research & Application 22,269-274 (1997).
[9] J. Kuang, X. Jiang, S. Quan, R. Chiu:A psychophysical study on the influence factors of color preference in photographic color reproduction. In:Image Quality and System Performance IIon Proceedings (2005)
[10] S. Fernandez, M. Fairchild, Preferred Color Reproduction of Images with unknown Colorimetry. (2001), pp. 274-279.
[11] H. Zeng, M. Luo, Preferred skin colours of Africans, Caucasians, and Orientals. (2011).
[12] R. Peng *et al.*:Preferred skin reproduction centres for different skin groups. In:Color and Imaging Conferenceon Proceedings (2020)
[13] M. Cao, M. Luo, G. Liu: "Preferred skin tones reproduction of three ethnic groups under different ambient lighting conditions." Color and Imaging Conference 2020,94-99 (2020).
[14] M. R. Luo: "The new preferred memory color (PMC) chart." Color Research & Application 49,564-576 (2024).
[15] CM-700d/600d Homepage, https://www.konicaminolta.com.cn/instruments/products/legacy/cm700d-600d/index.html, last accessed 2025/31 May
[16] J. de Rigal, M. L. Abella, F. Giron, L. Caisey, M. A. Lefebvre: "Development and validation of a new Skin Color Chart." Skin Res Technol 13,101-109 (2007).
[17] M. Osto, I. H. Hamzavi, H. W. Lim, I. Kohli: "Individual Typology Angle and Fitzpatrick Skin Phototypes are Not Equivalent in Photodermatology." Photochem Photobiol 98,127-129 (2022).
[18] X2D 100C - Inspiration in Every Detail Homepage, https://www.hasselblad.com/x-system/x2d-100c/, last accessed
[19] LEDCube customized lighting scene simulator-Thouslight Homepage, https://thouslite.cn/product_detail/124.html, last accessed 2025/31 May
[20] CS-2000/CS-2000A Spectroradiometer -Konica Minolta Homepage, https://www.konicaminolta.com.cn/instruments/products/legacy/cs2000/index.html, last accessed 2025/31 May
[21] CIE. (Central Bureau of the CIE, Vienna, 2001).
[22] M. R. Luo, G. Cui, B. Rigg: "The development of the CIE 2000 colour-difference formula: CIEDE2000." Color Research & Application 26,340-350 (2001).
[23] J. Lee, S. Yoo: "An Elliptical Boundary Model for Skin Color Detection." (2002).
[24] H. Zeng, M. Luo: "Skin Color Modeling of Digital Photographic Images." Journal of Imaging Science and Technology 55,030201 (2011).
[25] A. L. Cecala: "Psychophysics: A Practical Introduction (2nd Ed.)." J Undergrad Neurosci Educ 15,R21 (2016).
[26] A. L. Cecala: "Psychophysics: A Practical Introduction (2nd Ed.)."
[27] R. B. Burns:Experimental Psychology: Research Methods and Statistics. on Proceedings (1980)
[28] L. Changjun *et al.*: "Comprehensive color solutions: CAM16, CAT16, and CAM16 - UCS." Color Research and Application,42 (2017).
[29] A. Maydeu-Olivares, in Recent Developments on Structural Equation Models: Theory and Applications, K. van Montfort, J. Oud, A. Satorra, Eds. (Springer Netherlands, Dordrecht, 2004), pp. 41-67.
[30] S. Mrug: "Experimental Design And Statistics for Psychology: A First Course." The American Statistician 61,275 - 276 (2007).
[31] A. Alexandersson: "Graphing Confidence Ellipses: An Update of Ellip for Stata 8." Stata Journal 4,242-256 (2004).
[32] H. B. Mann, D. R. Whitney: "On a Test of Whether one of Two Random Variables is Stochastically Larger than the Other." The Annals of Mathematical Statistics 18,50-60 (1947).
[33] Lilliefors, W. Hubert: "On the Kolmogorov-Smirnov Test for Normality with Mean and Variance Unknown." Publications of the American Statistical Association 62,399-402 (1967).
[34] R. A. Fisher: "On a Distribution Yielding the Error Functions of Several Well Known Statistics. ." (1924).
[35] W. H. Kruskal, W. A. Wallis: "Taylor & Francis Online :: Use of Ranks in One-Criterion Variance Analysis - Journal of the American Statistical Association - Volume 47, Issue 260." Taylor & Francis.

. Author Information

Beijia Qin is a mater student in Zhejiang University, China. She studies about the subjective evaluation of skin color.

Yuechen Zhu is a postdoctor at Zhejiang University, China. She studies about the color adaptation transform.

Ming Ronnier Luo is a Qiushi Professor at the College of Optical Science and Engineering, Zhejiang University (China). He has published 800 peer reviewed papers in the fields of colour science, imaging science and illumination engineering. He is a Fellow of Imaging Science and Technology (IS&T). He has been an active member of International Commission on Illumination (CIE). He has received numerous awards, including the Judd 2017 Award and the Newton 2020 Award for his contribution in colour science research.